Electrochemical Carbon Dioxide Fixation to Thioesters Catalyzed by $[Mo_2Fe_6S_8(SEt)_9]^{3-}$

Nobutoshi Komeda,[§] Hirotaka Nagao,[†] Tatsuji Matsui,[§] Gin-ya Adachi,[§] and Koji Tanaka*,[†]

Contribution from the Institute for Molecular Science, Myodaiji, Okazaki 444, Japan, and Department of Applied Chemistry, Faculty of Engineering, Osaka University, Yamada-oka, Suita, Osaka 565, Japan. *Received October 15, 1991*

Abstract: A controlled potential electrolysis at −1.55 V versus SCE of CO_2-saturated CH_3CN containing $(Et_4N)_3[Mo_2Fe_6S_8(SEt)_9]$, $CH_3C(O)SEt$, Bu_4NBF_4, and Molecular Sieve 3A as a desiccant produced $CH_3C(O)COO^-$ with a current efficiency of 27%. Similar electrolysis using $C_2H_5C(O)SEt$ and $C_6H_5C(O)SEt$ also catalytically afforded $C_2H_5C(O)COO^-$ and $C_6H_5C(O)COO^-$ with current efficiencies of 49 and 13%, respectively. These reactions are strongly inhibited by the presence of not only H_2O but also excess EtS^-. Strong acylating agents such as acetyl chloride, acetic anhydride, acetyl sulfide, and acetylimidazole in place of $CH_3C(O)SEt$ caused decomposition of $[Mo_2Fe_6S_8(SEt)_9]^{3-}$, and no $CH_3C(O)COO^-$ was formed under the same electrolysis conditions.

Introduction

Much attention has been paid to carbon dioxide fixation in connection with not only an increase of the concentration of CO_2 in the atmosphere but also as a possible carbon source for organic chemicals. Electrochemical CO_2 reduction takes place at fairly negative potentials (E^0 = −2.21 V versus SCE).[1] Therefore, activation of CO_2 has been conducted by using various transition metal complexes to decrease the high overpotential of the reduction, and a variety of transition metal complexes have been proven to catalyze electrochemical reduction of CO_2 to CO and/or HCOOH.[2] From the standpoint of utilization of CO_2 as a C_1 building block, carbon–carbon bond formation by carbon dioxide fixation to organic molecules may be much more important than the reduction of CO_2. A catalytic incorporation of CO_2 to alkynes and dienes activated on coordinatively unsaturated metal centers has been well documented.[3] In biological systems, CO_2 in fixed to the α- and β-carbons of the carbonyl group of organic molecules to form hydroxy or keto acids,[4] although it has not bee elucidated whether CO_2 or substrates are mainly activated by enzymes. The reductive carboxylic acid cycle by photosynthetic bacteria[5] contributes to the conversion of CO_2 to precursors of fatty acids, amino acids, and porphyrins. Four molecules of CO_2 are fixed in one turn; two of them are fixed to β-carbons of the carbonyl groups of pyruvate and α-keto glutarate to produce oxalacetate and isocitrate (eq 1), and the other two molecules of CO_2 are introduced to the α-carbons of carbonyl groups of acetyl coenzyme A and succinyl coenzyme A to generate pyruvate and α-keto glutarate respectively (eq 2), where reduced ferredoxins, generated photochemically, function as electron donors. In connection with the CO_2 fixation of eq 1, a catalytic β-keto acid formation by artificial CO_2 fixation has been achieved by electrochemical carboxylation of ketones coupled with NO_2^- reduction by $[Fe_4S_4(SPh)_4]^{2-}$ (eq 3).[6] With respect to the α-keto acid formation by nonenzymatic CO_2 fixation, formation of $C_6H_5CH_2C(O)COO^-$ has been proposed as a precursor of $C_6H_5CH_2CH(NH_2)COO^-$ (0.3% yield) resulting from the reaction of $C_6H_5CH_2C(O)SC_8H_{17}$ with CO_2 in the presence of $[Fe(S_2C_2Ph_2)_2]_2$, $Na_2S_2O_4$, $NaHCO_3$, and NH_3 (eq 4).[7] Furthermore, $CH_3C(O)SC_6H_4CH_3$ is also converted to $CH_3C(O)COO^-$ in a 1.3% yield under similar reaction conditions.[8] In those reactions, CO_2 is fixed at positively polarized carbonyl carbons. However, it has not been elucidated whether CO_2 or thioester is activated, and the yield of α-keto acid is quite low. A catalytic formation of

$$RCH_2C(O)COOH + CO_2 \rightarrow RCH(COOH)C(O)COOH \quad (1)$$
$$(R = H, HOOCCH_2)$$

$$RC(O)SCoA + CO_2 + 2e^- \rightarrow RC(O)COO^- + CoAS^- \quad (2)$$
$$(R = CH_3, HOOCCH_2CH_2;\ CoA = \text{coenzyme A})$$

$$2NO_2^- + 8RC(O)CH_3 + 8CO_2 + 6e^- \rightarrow N_2 + 8RC(O)CH_2COO^- + 4H_2O \quad (3)$$
$$(R = C_6H_5, CH_3)$$

$$C_6H_5CH_2C(O)SC_8H_{17} + CO_2 + 2e^- \xrightarrow[-SC_8H_{17}]{} [C_6H_5CH_2C(O)COO^-] \rightsquigarrow C_6H_5CH_2CH(NH_2)COO^- \quad (4)$$

[§] Osaka University.
[†] Institute for Molecular Science.

(1) (a) Amatore, C.; Saveant, J.-M. *J. Am. Chem. Soc.* **1981**, *103*, 5021. (b) Gressin, J.-C.; Michelet, D.; Nadjo, L.; Saveant, J.-M. *Nouv. J. Chim.* **1979**, *3*, 545.

(2) (a) Atoguchi, T.; Aramata, A.; Kazusaka, A.; Enyo, M. *J. Chem. Soc., Chem. Commun.* **1991**, 156. (b) Tsai, J. C.; Khan, M. A.; Nicholas, K. M. *Organometallics* **1991**, *10*, 29. (c) Fujita, E.; Creutz, C.; Sutin, N.; Szalda, D. J. *J. Am. Chem. Soc.* **1991**, *113*, 343. (d) Ishida, H.; Fujiki, K.; Ohba, T.; Ohkubo, K.; Tanaka, K.; Terada, T.; Tanaka, T. *J. Chem. Soc., Dalton Trans.* **1990**, 2155. (e) Pugh, J. R.; Bruce, M. R. M.; Sullivan, B. P.; Meyer, T. J. *Inorg. Chem.* **1991**, *30*, 86. (f) Ruiz, J.; Guerchais, V.; Astruc, D. *J. Chem. Soc., Chem. Commun.* **1989**, 812. (g) Tomohiro, T.; Uoto, K.; Okuno, H. *J. Chem. Soc., Chem. Commun.* **1990**, 194. (h) Ishida, H.; Terada, T.; Tanaka, K.; Tanaka, T. *Inorg. Chem.* **1990**, *29*, 905. (i) Silavwe, N. D.; Goldman, A. S.; Ritter, R.; Tyler, D. R. *Inorg. Chem.* **1989**, *28*, 1231. (j) Hurrell, H. C.; Mogstad, A. L.; Usifer, D. A.; Potts, K. T.; Abruna, H. D. *Inorg. Chem.* **1989**, *28*, 1080 and references therein.

(3) (a) Inoue, Y.; Sasaki, Y.; Hashimoto, H. *Bull. Chem. Soc. Jpn.* **1978**, *51*, 2375. (b) Inoue, Y.; Hibi, T.; Satake, M.; Hashimoto, H. *J. Chem. Soc., Chem. Commun.* **1979**, 982. (d) Inoue, Y.; Itoh, Y.; Kazama, H.; Hashimoto, H. *Bull. Chem. Soc. Jpn.* **1980**, *53*, 3329. (e) Binger, P.; Weintz, H.-J. *Chem. Ber.* **1984**, *117*, 654. (f) Walther, D.; Schonberg, H.; Dinjus, E.; Sieler, J. *J. Organomet. Chem.* **1987**, *334*, 377. (g) Tsuda, T.; Morikawa, S.; Sumiya, R.; Saegusa, T. *J. Org. Chem.* **1988**, *53*, 3140. (f) Tsuda, T.; Morikawa, S.; Saegusa, T. *J. Chem. Soc., Chem. Commun.* **1989**, 9.

(4) Inoue, S.; Yamazaki, N., Eds. *The Organic and Bioorganic Chemistry of Carbon Dioxide*; Halstead Press: New York, 1982. Friedli, H.; Lotscher, H.; Siegenthaler, U.; Stauffer, B. *Nature (London)* **1986**, *324*, 237.

(5) (a) Evans, M. C. W.; Buchanan, B. B.; Arnon, D. I. *Proc. Natl. Acad. Sci. U.S.A.* **1966**, *55*, 928. (b) Kusai, A.; Yamanaka, T. *Biochim. Biophys. Acta* **1973**, *292*, 621. (c) Bachofen, R.; Buchanan, B. B.; Arnon, D. I. *Biochemistry* **1964**, *51*, 690. (d) Buchanan, B. B.; Bachofen, R.; Arnon, D. I. *Biochemistry* **1964**, *52*, 839. (e) Evans, M. C. W.; Buchanan, B. B.; Arnon, D. I. *Biochemistry* **1966**, *55*, 928. (f) Evans, M. C. W. *Biochem. Biophys. Res. Commun.* **1968**, *33*, 146. (g) Gottschalk, G.; Chowdhury, A. A. *FEBS Lett.* **1969**, *2*, 342. (h) Thauer, R. K.; Rupprecht, E.; Jungermann, K. *FEBS Lett.* **1970**, *8*, 304.

(6) (a) Tanaka, K.; Wakita, R.; Tanaka, T. *Chem. Lett.* **1987**, 1951. (b) Tanaka, K.; Wakita, R.; Tanaka, T. *J. Am. Chem. Soc.* **1989**, *111*, 2428.

(7) (a) Nakajima, T.; Yabushita, Y.; Tabushi, I. *Nature (London)* **1975**, *256*, 60. (b) Tabushi, I.; Yabushita, Y.; Nakajima, T. *Tetetrahedron Lett.* **1976**, 4343.

(8) Kubota, Y.; Kodaka, M.; Tomohiro, T.; Okuno, H. *Chem. Express* **1991**, 487.

0002-7863/92/1514-3625$03.00/0

α-keto acids by nonenzymatic CO_2 fixation, therefore, is highly desired in the viewpoint of mimicking of the novel CO_2 assimilation as a model reaction of pyruvate synthase (eq 2). This paper describes α-keto acid formation by artificial CO_2 fixation to RC(O)SEt (R = CH_3, C_2H_5, C_6H_5) as a model of coenzyme A catalyzed by $[Mo_2Fe_6S_8(SEt)_9]^{3-}$ under controlled potential electrolysis conditions, and a possible reaction mechanism is presented. Part of this work has been reported elsewhere.[9]

Experimental Section

Materials. $(Et_4N)_3[Mo_2Fe_6S_8(SEt)_9]$,[10] $(Bu_4N)_3[Mo_2Fe_6S_8(SPh)_9]$,[10] $(Et_4N)_2[Fe_4S_4(SCH_2Ph)_4]$,[11] and $(Bu_4N)_2[Fe_4S_4(SPh)_4]$[12] were prepared according to literature procedures. Commercially available guaranteed reagent grade Bu_4NBF_4, $CH_3C(O)COOH$, $C_2H_5C(O)COOH$, and $C_6H_5C(O)COOH$ were used, and other reaction products such as $CH_3C(O)CH_2C(O)SEt$[13] and $CH_3OC(O)CH_2C(O)SEt$[14] were prepared. Ethyl thioacetate ($CH_3C(O)SEt$) was synthesized as follows. Acetyl chloride was added dropwise to a suspension of sodium ethanethiolate in dry diethyl ether (1:1:1 molar ratio); the suspension was stirred for 3 h at room temperature. After sodium chloride in the reaction mixture was removed by filtration, the filtrate was washed with water to remove CH_3COOH and EtSH, and the ether layer was dried with Na_2SO_4. Ethyl thioacetate was obtained by fractional distillation of the solution (bp 389 K). Similarly, ethyl thiopropionate (bp 399 K), ethyl thiobenzoate (bp 419 K (31 mmHg)), and *n*-propyl thioacetate (bp 413 K) were prepared. Acetonitrile was refluxed with CaH_2 for 48 h, followed by distillation over P_2O_5 three times and over CaH_2, and then stored over Molecular Sieve 3A under N_2 atmosphere. Carbon dioxide was dried by passing through a glass tube packed with P_2O_5. Molecular Sieve 3A was dehydrated at 523 K under reduced pressure before use.

Physical Measurements. Electronic absorption spectra were measured with a Union SM-401 spectrophotometer. Spectroelectrochemical experiments were carried out by using an optically transparent thin layer electrode (OTTLE), consisting of a Pt-gauze electrode in a 0.5-mm quartz cuvette, a Pt wire auxiliary electrode, and a saturated calomel reference electrode (SCE).[15] Electrochemical measurements were performed in a Pyrex cell equipped with a glassy carbon working electrode, a Pt auxiliary electrode, a SCE, and a nozzle for bubbling N_2 or CO_2. Cyclic voltammograms were obtained by use of a Hokuto Denko HR-101B potentiostat, a Hokuto Denko HB-107A function generator, and a Yokogawa Electric Inc. 3077 X–Y recorder.

Carbon Dioxide Fixation. Carbon dioxide fixation to RC(O)SEt catalyzed by $(Et_4N)_3[Mo_2Fe_6S_8(SEt)_9]$ was carried out under controlled potential electrolysis conditions in CH_3CN. The electrolysis cell consisted of three compartments: one for a glassy carbon working electrode, the second for a platinum auxiliary electrode, which is separated from the working electrode cell by a cation exchange membrane (Nafion film), and the third for a SCE reference electrode.[16] The volumes of these compartments were 39, 25, and 10 cm^3, respectively, and the working electrode compartment was connected to a volumetric flask filled with liquid paraffin by the stainless steel tube. Molecular Sieve 3A and a CH_3CN solution of $(Et_4N)_3[Mo_2Fe_6S_8(SEt)_9]$, Bu_4NBF_4, and RC(O)SEt were introduced into the working electrode compartment under N_2 atmosphere. Then CH_3CN in the working electrode compartment and liquid paraffin in the volumetric flask were saturated with CO_2 by bubbling of CO_2 for 30 min; the CH_3CN solution was stirred magnetically for 30 min to attain the thermal equilibrium of CO_2. Carbon dioxide fixation was started by applying a given electrolysis potential to a glassy carbon working electrode with a potentiostat (Hokuto Denko HA-301); the electricity consumed in the electrolysis was measured with a Hokuto Denko HF-201 coulomb meter.

Product Analysis. At a fixed interval of electricity consumed in the electrolysis, each 0.1-cm^3 portion of gas was sampled from the gaseous phases of both the working electrode compartment and the volumetric flask with a pressure-locked syringe (Precision Sampling). Gaseous products were analyzed on a Shimadzu GC-3BT gas chromatograph equipped with a 2.0-m column filled with Molecular Sieve 13X at 343 K using He (0.8 kg/cm^2) as a carrier gas. The analysis of reactants and products in the solution was performed by sampling each 0.1-cm^3 portion from the working electrode compartment through a septum cap by syringe techniques. After the sampled solution was mixed with the same volume of water, the mixture was centrifuged, followed by filtration with a membrane filter to remove insoluble materials such as clusters and Molecular Sieve 3A. Reaction products in the filtrate were analyzed by not only HPLC with a column packed with Shodex Ionpack KC-811 at 313 K using an aqueous solution of 0.2% H_3PO_4–10% EtOH as a mobile phase (0.8 cm^3/min), but also a Shimadzu Isotachophoretic Analyzer IP-2A using aqueous HCl/β-alanine (0.1 mol/dm^3) and caproic acid (0.01 mol/dm^3) solutions as leading and terminal electrolytes, respectively. After the electrolysis, an aqueous HCl solution (0.1 N, 10 cm^3) was added to oily residue obtained by evaporation of the solvent in vacuo to decompose the cluster at 273 K. Then reaction products were extracted with diethyl ether (2 cm^3) and converted into the corresponding methyl esters by treatment with CH_2N_2. The ether solution thus obtained was analyzed by a Shimadzu GCMS-QP1000EX equipped with a 20-m capillary column at 313–573 K using He as a carrier gas; the reaction products were identified by comparing retention times and mass fragments with those of authentic samples.

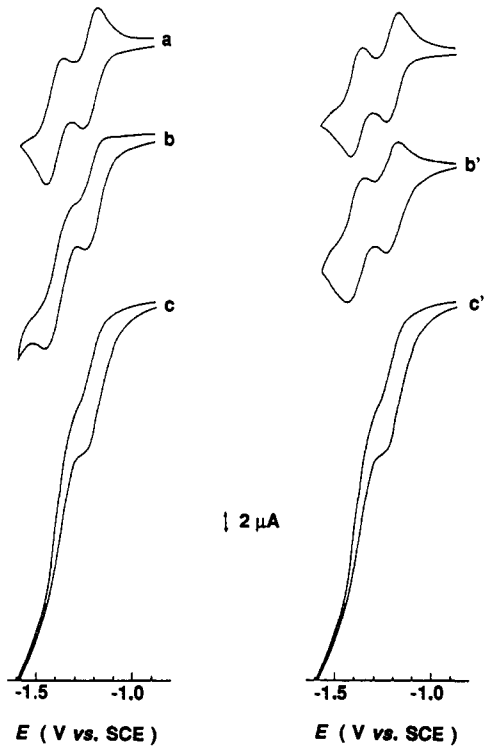

Figure 1. Cyclic voltammograms of $(Et_4N)_3[Mo_2Fe_6S_8(SEt)_9]$ (2.4 mmol/dm^3) in the absence of (a) and presence of CO_2 (bubbled for 10 min) (b) or $CH_3C(O)SEt$ (0.6 mol/dm^3) (b'), and those in the presence of both CO_2 and $CH_3C(O)SEt$ (c and c') in CH_3CN (8.0 cm^3) containing Molecular Sieve 3A and Bu_4NBF_4 (0.5 mol/dm^3); dE/dt = 5.0 mV/s.

Results and Discussion

Interaction between CO_2 and $[Mo_2Fe_6S_8(SEt)_9]^{3-}$. A cyclic voltammogram (CV) of $(Et_4N)_3[Mo_2Fe_6S_8(SEt)_9]$ (2.4 mmol/dm^3) shows the (3–/4–) and (4–/5–) redox couples at $E_{1/2}$ = −1.27 and −1.46 V versus SCE, respectively, at 5 mV/s in dry CH_3CN (Figure 1a). The (3–/4–) redox couple of the cluster is not largely influenced by bubbling of CO_2 into the solution, although the cathodic peak current of the (4–/5–) redox couple slightly increases compared with that in a N_2 atmosphere (Figure 1b). Removal of CO_2 from the CH_3CN solution by bubbling of N_2 for 30 min regenerated the CV of $[Mo_2Fe_6S_8(SEt)_9]^{3-}$ (Figure 1a). Such a difference in the CV in the absence and the presence of CO_2 was observed only in a slow potential sweep, because the CV of the cluster at 100 mV/s under CO_2 was consistent with that in a N_2 atmosphere at the same sweep rate. These results indicate that $[Mo_2Fe_6S_8(SEt)_9]^{5-}$ weakly interacts with CO_2, and

(9) Tanaka, K.; Matsui, T.; Tanaka, T. *J. Am. Chem. Soc.* **1989**, *111*, 3062.
(10) Christou, G.; Garner, C. D. *J. Chem. Soc., Dalton Trans.* **1980**, 2354.
(11) Averill, B. A.; Herskovitz, T.; Holm, R. H.; Ibers, J. A. *J. Am. Chem. Soc.* **1973**, *95*, 3523.
(12) Que, L.; Bobrik, M. A.; Ibers, J. A.; Holm, R. H. *J. Am. Chem. Soc.* **1974**, *96*, 4168.
(13) (a) Motoki, S.; Sato, T. *Bull. Chem. Soc. Jpn.* **1969**, *42*, 1322. (b) Baker, R. B.; Reid, E. E. *J. Am. Chem. Soc.* **1929**, *51*, 1567.
(14) Imamoto, T.; Kodera, M.; Yokoyama, M. *Bull. Chem. Soc. Jpn.* **1982**, *55*, 2303.
(15) Lexa, D.; Savent, J. M.; Zickler, J. J. *J. Am. Chem. Soc.* **1977**, *99*, 2786.
(16) Tanaka, K.; Honjo, M.; Tanaka, T. *J. Inorg. Biochem.* **1984**, *22*, 187.

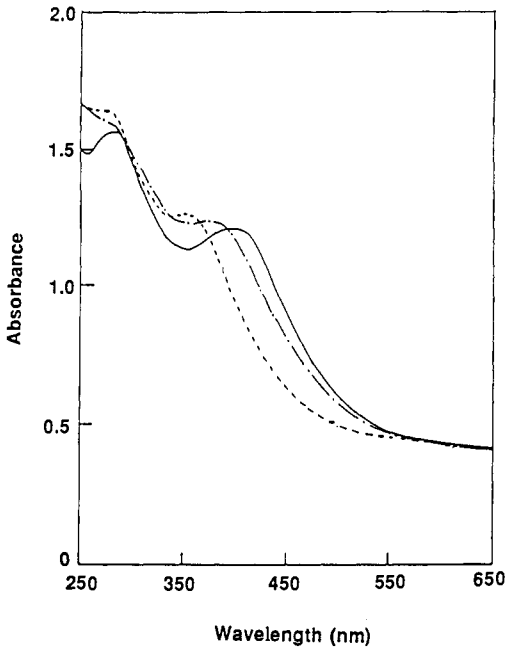

Figure 2. Electronic absorption spectra of $(Et_4N)_3[Mo_2Fe_6S_8(SEt)_9]$ (0.14 mmol/dm^3) (—) and $[Mo_2Fe_6S_8(SEt)_9]^{5-}$ produced at −1.55 V versus SCE in the absence (---) and presence of CO_2 (bubbled for 15 min) (---) in CH_3CN.

the process is relatively slow. Addition of $CH_3C(O)SEt$ (0.6 mol/dm^3) to the CH_3CN solution of $[Mo_2Fe_6S_8(SEt)_9]^{3-}$ under CO_2 atmosphere causes a strong irreversible cathodic current at potentials more negative than about −1.4 V. Alternatively, the CV of $[Mo_2Fe_6S_8(SEt)_9]^{3-}$ under N_2 is hardly affected by addition of $CH_3C(O)SEt$ (Figure 1b′). Thus, $[Mo_2Fe_6S_8(SEt)_9]^{n-}$ (n = 3, 4, 5) does not show any interactions with $CH_3C(O)SEt$ in a CV time scale. The agreement of the threshold potential of the irreversible cathodic current (Figure 1c) with that of the (4−/5−) cathodic wave of the cluster (Figure 1, a and b) implies a reaction of $CH_3C(O)SEt$ with CO_2 activated by $[Mo_2Fe_6S_8(SEt)_9]^{5-}$. It should be noticed that $(Bu_4N)_3[Mo_2Fe_6S_8(SPh)_9]$ also shows the (3−/4−) and (4−/5−) redox couples at $E_{1/2}$ = −0.91 and −1.09 V in CH_3CN under N_2, and the cathodic wave of the (4−/5−) couple slightly increased under CO_2 atmosphere at 10 mV/s, similar to the $[Mo_2Fe_6S_8(SEt)_9]^{4-/5-}$ redox couple under CO_2 atmosphere. No irreversible cathodic current, however, was observed in a CV of $(Bu_4N)_3[Mo_2Fe_6S_8(SPh)_9]$ in the presence of $CH_3C(O)SEt$ in CO_2-saturated CH_3CN at 10 mV/s. Therefore, $[Mo_2Fe_6S_8(SEt)_9]^{3-}$ seems to be much superior to $[Mo_2Fe_6S_8(SPh)_9]^{3-}$ with regard to the ability to catalyze a reaction of CO_2 with $CH_3C(O)SEt$. Furthermore, neither CO_2 nor $CH_3C(O)SEt$ had any influence on the CV of $(Et_4N)_2[Fe_4S_4(SEt)_4]$ at a sweep rate of 10 mV/s in CH_3CN. Thus, only the $(Et_4N)_3[Mo_2Fe_6S_8(SEt)_9]/CO_2/CH_3C(O)SEt$ system showed an irreversible cathodic current in cyclic voltammograms.

The interaction between $[Mo_2Fe_6S_8(SEt)_9]^{3-}$ and CO_2 was also observed in the electronic absorption spectra in CH_3CN; $(Et_4N)_3[Mo_2Fe_6S_8(SEt)_9]$ shows two absorption bands centered at 280 and 400 nm (a solid line in Figure 2), the latter of which is an LMCT band from the ethanethiolate ligand to metals. The LMCT band shifts from 400 to 350 nm (broken line in Figure 2) upon electrochemical reduction of $[Mo_2Fe_6S_8(SEt)_9]^{3-}$ to $[Mo_2Fe_6S_8(SEt)_9]^{5-}$ at −1.55 V under N_2 (broken line). The electrolysis of $(Et_4N)_3[Mo_2Fe_6S_8(SEt)_9]$ at the same potential in CO_2-saturated CH_3CN exhibits the LMCT band around 380 nm (dotted line), which is apparently different from those of $[Mo_2Fe_6S_8(SEt)_9]^{3-}$ and $[Mo_2Fe_6S_8(SEt)_9]^{5-}$.

Carbon Dioxide Fixation to RC(O)SEt (R = CH_3, C_2H_5, C_6H_5). In accordance with the observation that no irreversible cathodic current is observed in the CV of a CH_3CN solution of $(Bu_4N)_3[Mo_2Fe_6S_8(SPh)_9]$ in the presence of $CH_3C(O)SEt$ under CO_2, only two-electron reduction of $[Mo_2Fe_6S_8(SPh)_9]^{3-}$ took place

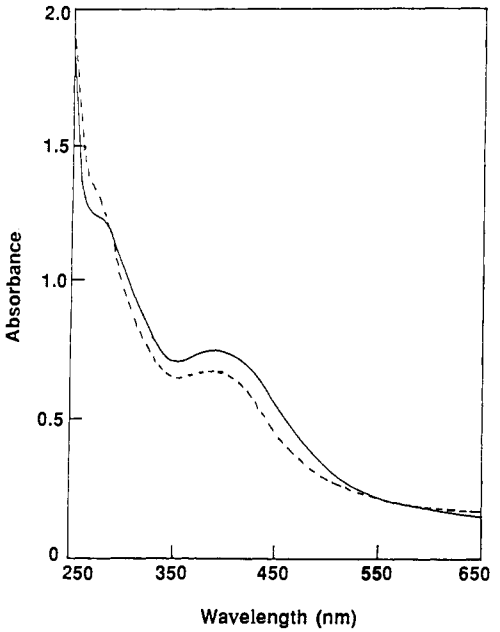

Figure 3. Electronic absorption spectra of $[Mo_2Fe_6S_8(SEt)_9]^{3-}$ (0.11 mmol/dm^3) before (—) and after (---) the CO_2 fixation in CH_3CN.

in the controlled potential electrolysis of a CH_3CN solution (15 cm^3) containing $(Bu_4N)_3[Mo_2Fe_6S_8(SPh)_9]$ (30 μmol), $CH_3C(O)SEt$ (7.6 mmol), Bu_4NBF_4 (2.0 mmol), and Molecular Sieve 3A (0.4 g) at −1.50 V under CO_2. A similar controlled potential electrolysis by using $(Et_4N)_3[Mo_2Fe_6S_8(SEt)_9]$ in place of $(Bu_4N)_3[Mo_2Fe_6S_8(SPh)_9]$ at −1.55 V produced $CH_3C(O)COO^-$ (eq 5) together with $HCOO^-$ (eq 6). In the initial stage,

$$CH_3C(O)SEt + CO_2 + 2e^- \rightarrow CH_3C(O)COO^- + EtS^- \quad (5)$$

$$H^+ + CO_2 + 2e^- \rightarrow HCOO^- \quad (6)$$

$CH_3C(O)COO^-$ and $HCOO^-$ were generated with time with a current efficiency of 27% and 11%, respectively. The cathodic current, however, gradually decreased, and the amount of $CH_3C(O)COO^-$ leveled off after 90 C passed in the electrolysis. The electrochemical reoxidation of the final solution at −1.0 V (after 90 C passed in the electrolysis) regenerated the electronic absorption spectrum of $[Mo_2Fe_6S_8(SEt)_9]^{3-}$ with an optical density of 90% of the LMCT band at 450 nm (Figure 3). This result strongly suggests that $[Mo_2Fe_6S_8(SEt)_9]^{5-}$ is maintained during the electrolysis, and the cessation of the reaction after 90 C does not result from decomposition of $[Mo_2Fe_6S_8(SEt)_9]^{5-}$.

The reaction (eq 5) is essentially the same as the CO_2 fixation by pyruvate synthase (eq 2), although $HCOO^-$ (eq 6) is not formed in the biological CO_2 fixation. In the present study, unavoidable water in the solvent, of course, is a possible proton source of $HCOO^-$ (eq 6). Water, however, showed a strong inhibitory effect on the formation of $CH_3C(O)COO^-$ (eq 5). The current efficiency for $CH_3C(O)COO^-$ (eq 5) decreased to less than 1.0% in case an insufficient dehydration of CH_3CN was used as the solvent, and H_2 became the major product accompanied by $HCOO^-$ formation. Furthermore, hydrolysis of $CH_3C(O)SEt$ occurred in the electrolysis and $CH_3C(O)O^-$ was confirmed in the reaction mixture. It has been reported that Bu_4N^+ used as an electrolyte provides a proton for formation of $HCOO^-$ in an electrochemical reduction of CO_2 catalyzed by $[Fe_4S_4(SR)_4]^{2-}$ (R = Et, CH_2Ph) and $[Mo_2Fe_6S_8(SEt)_9]^{3-}$ at −2.0 V versus SCE in DMF.[17] Deprotonation decomposition of Bu_4N^+ (eq 7), however, may be

$$(C_4H_5)_4N^+ \rightarrow (C_4H_5)_3N + C_2H_5CH{=}CH_2 + H^+ \quad (7)$$

(17) (a) Tezuka, M.; Yajima, T.; Tsutuya, A.; Matsumoto, Y.; Uchida, Y.; Hidai, M. *J. Am. Chem. Soc.* **1982**, *104*, 6835. (b) Nakazawa, M.; Mizobe, U.; Matsumoto, Y.; Uchida, Y.; Tezuka, M.; Hidai, M. *Bull. Chem. Soc. Jpn.* **1986**, *59*, 809.

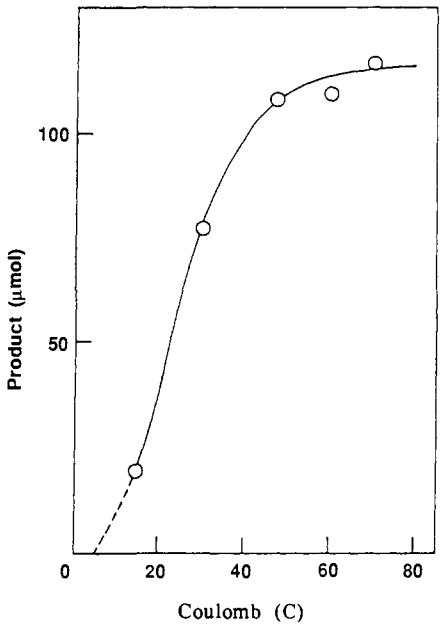

Figure 4. Electrochemical CO_2 fixation in the presence of $(Et_4N)_3[Mo_2Fe_6S_8(SEt)_9]$ (23 μmol), $C_2H_5C(O)SEt$ (7.6 mmol), Bu_4NBF_4 (1.5 mmol), and Molecular Sieve 3A in CO_2-saturated CH_3CN (15 cm^3) at −1.65 V versus SCE.

ignored in the present reaction conditions, since neither Bu_3N nor C_4H_8 was identified in the reaction mixture by GC analysis. On the other hand, $C_6H_5C(O)CH_3$ has been shown to undergo a deprotonation reaction by $[Fe_4S_4(SPh)_4]^{2-}$ in CO_2-saturated CH_3CN to afford not only $C_6H_5C(O)CH_2COO^-$ but also $HCOO^-$ under a controlled potential electrolysis at −2.0 V (eq 8).[3] In

$$C_6H_5C(O)CH_3 + 2CO_2 + 2e^- \rightarrow C_6H_5C(O)CH_2COO^- + HCOO^- \quad (8)$$

addition, electrolysis of $CH_3C(O)CH_3$ under similar conditions predominantly produces $CH_3C(O)CH_2C(CH_3)_2OH$.[3] In accordance with these reactions, $CH_3OC(O)CH_2C(O)SC_2H_5$ (3.4 μmol)[18] and $CH_3C(O)CH_2C(O)SC_2H_5$ (11 μmol) were identified together with $CH_3C(O)COOCH_3$ in the present reaction after treatment of the crude products with CH_2N_2 (see Experimental Section). Based on the fact that $CH_3C(O)SEt$ is not reduced up to −1.90 V by a glassy carbon electrode, the formation of $HCOO^-$ (eq 6) may be associated with deprotonation of $CH_3C(O)SEt$ catalyzed by $[Mo_2Fe_6S_8(SEt)_9]^{5-}$, and $^-OOCCH_2C(O)SEt$ and $CH_3C(O)CH_2C(O)SEt$ are formed by reactions of the resulting $^-CH_2C(O)SEt$ with CO_2 (eq 9) and $CH_3C(O)SEt$ (eq 10).

$$CH_3C(O)SEt + 2e^- + 2CO_2 \rightarrow {}^-OOCCH_2C(O)SEt + HCOO^- \quad (9)$$

$$2CH_3C(O)SEt + 2e^- + CO_2 \rightarrow CH_3C(O)CH_2C(O)SEt + EtS^- + HCOO^- \quad (10)$$

The controlled potential electrolysis of a CO_2-saturated CH_3CN solution containing $(Et_4N)_3[Mo_2Fe_6S_8(SEt)_9]$ (23 μmol), $C_2H_5C(O)SEt$ (7.6 mmol), and Molecular Sieve 3A at −1.65 V versus SCE also produced $C_2H_5C(O)COO^-$ (eq 11). The in-

$$C_2H_5C(O)SEt + CO_2 + 2e^- \rightarrow C_2H_5C(O)COO^- + EtS^- \quad (11)$$

duction period observed in the initial stage of the electrolysis (Figure 4) indicates that the reaction (eq 11) takes place after two-electron reduction of $[Mo_2Fe_6S_8(SEt)_9]^{3-}$, and the amount of $C_2H_5C(O)COO^-$ increases with a current efficiency of 49.3% up to about 50 C. The current efficiency for $C_2H_5C(O)COO^-$ is fairly improved compared with $CH_3C(O)COO^-$, although the

(18) The formation of $EtSC(O)CH_2COOH$ was also confirmed by HPLC, and the amount of it was 46 μmol, after 80 C passed in the electrolysis.

Scheme I

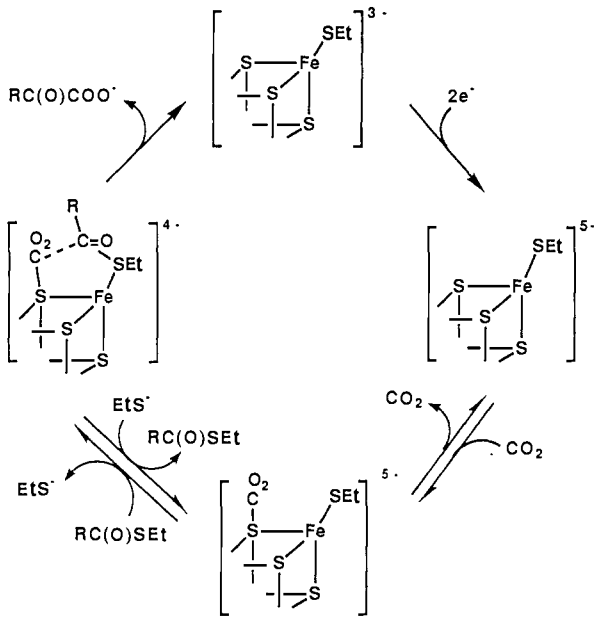

reaction still stopped after about 600% of $C_2H_5C(O)COO^-$ was formed (based on the cluster). In this reaction, a small amount of $HCOO^-$ was also formed, and after treatment of the crude product with CH_2N_2, trace amounts of $CH_3CH(COOCH_3)C(O)SEt$ and $C_2H_5C(O)CH(CH_3)C(O)SEt$ as carboxylation and Claisen condensation products of $C_2H_5C(O)SEt$ were confirmed. It should be noticed that prolonged electrolysis of $[Mo_2Fe_6S_8(SEt)_9]^{3-}$ in the absence of free EtS^- results in a gradual decomposition in DMF under CO_2.[17] In the present study, reoxidation of the final solution (after the CO_2 fixation stopped) at −0.9 V almost completely regenerates the electronic absorption spectrum of $[Mo_2Fe_6S_8(SEt)_9]^{3-}$. This result implies that an accumulation of EtS^- formed in reactions of eq 5 and 11 results in not only stability of $[Mo_2Fe_6S_8(SEt)_9]^{5-}$ during the electrolysis but also cessation of those reactions. In fact, when the electrolysis of $(Et_4N)_3[Mo_2Fe_6S_8(SEt)_9]$ was conducted in the presence of $C_2H_5C(O)SEt$ and 6 M excess of the Et_4N^+ salt of EtS^- in CO_2-saturated CH_3CN at −1.60 V, a cathodic current rapidly decreased after two-electron reduction of $[Mo_2Fe_6S_8(SEt)_9]^{3-}$, and the current efficiency for $C_2H_5C(O)COO^-$ was as low as 0.4%. It, therefore, is concluded that free EtS^- as a by-product of the CO_2 fixation to $C_2H_5C(O)SEt$ stabilizes $[Mo_2Fe_6S_8(SEt)_9]^{5-}$ but strongly inhibits α-keto acid formation (eq 5 and 11).

The controlled potential electrolysis at −1.55 V of a dry CH_3CN solution containing $[Mo_2Fe_6S_8(SEt)_9]^{3-}$, $C_6H_5C(O)SEt$, Bu_4NBF_4, and Molecular Sieve 3A under CO_2 atmosphere also produced $C_6H_5C(O)COO^-$ with a current efficiency of 13% (eq 12). The

$$C_6H_5C(O)SEt + CO_2 + 2e^- \rightarrow C_6H_5C(O)COO^- + EtS^- \quad (12)$$

absence of $HCOO^-$ in the reaction mixture adds strong support for the view that $CH_3C(O)SEt$ and $C_2H_5C(O)SEt$ play a role in the proton source for $HCOO^-$ formation under anhydrous conditions. In contrast to $RC(O)SEt$ and $RC(O)COO^-$ (R = CH_3, C_2H_5), not only $C_6H_5C(O)SEt$ but also $C_6H_5C(O)COO^-$ undergoes a slow irreversible reduction on a glassy carbon electrode at potentials more negative than −1.55 V versus SCE. Low current efficiency for the $C_6H_5C(O)COO^-$ formation (eq 12) compared with that of $RC(O)COO^-$ (R = CH_3, C_2H_5) may result from further irreversible reduction of $C_6H_5C(O)COO^-$ on a glassy carbon electrode, since $C_6H_5C(O)COO^-$ was not formed in the electrolysis of $C_6H_5C(O)SEt$ by using a glassy carbon electrode at −1.60 V in CH_3CN under CO_2 atmosphere.

It should be noticed that $CH_3CC(O)COO^-$ was not produced in the controlled potential electrolysis of a CH_3CN solution (15 cm^3) containing $(Et_4N)_2[Fe_4S_4(SCH_2Ph)_4]$ (37 μmol) and $CH_3C(O)SEt$ (9.6 mmol) at −1.50 V under CO_2. On the other

hand, the same electrolysis at −2.0 V gave a trace amount of $CH_3C(O)COO^-$ (1.3 μmol) with a current efficiency of 0.1%. Although $[Fe_4S_4(SCH_2Ph)_4]^{2-}$ shows only one stable (2−/3−) redox couple in CH_3CN, it may be reduced to the unstable (4−) state at −2.0 V from analogy with the $[Fe_4S_4(SPh)_4]^{2-/3-/4-}$ redox couples. This assumption implies that two-electron reduced Fe_4S_4 clusters also have the ability to catalyze the CO_2 fixation to thioesters, although $[Fe_4S_4(SCH_2Ph)_4]^{4-}$ is much more unstable than $[Mo_2Fe_6S_8(SEt)_9]^{5-}$.

Singularity of $[Mo_2Fe_6S_8(SEt)_9]^{3-}$ and RC(O)SEt in α-Keto Acid Formation. In the present CO_2 fixation, RC(O)SEt (R = CH_3, C_2H_5, and C_6H_5) behaves as an acylating agent of CO_2 in the presence of $[Mo_2Fe_6S_8(SEt)_9]^{5-}$. On the other hand, strong acylating agents such as acetyl chloride, acetic anhydride, acetyl sulfide, and acetylimidazole in place of ethyl thioacetate resulted in decolorization of $[Mo_2Fe_6S_8(SEt)_9]^{3-}$ during the electrolysis at −1.50 V under CO_2, and CH_4 was produced as the main product without generating $CH_3C(O)COO^-$. The electrolysis of $(Et_4N)_3[Mo_2Fe_6S_8(SEt)_9]$ (30 μmol) in the presence of $CH_3C(O)Cl$ (7 mmol) and Bu_4NBr in $^{13}CO_2$-saturated CH_3CN evolved only $^{12}CH_4$ (analyzed by GC–MS). Thus, CH_4 is the degradation product of $CH_3C(O)Cl$ and excess $CH_3C(O)Cl$ decomposes $[Mo_2Fe_6S_8(SEt)_9]^{3-}$ under the experimental conditions.[19] Thus, RC(O)SR′ as a model of acetyl coenzyme A seems to have a special meaning in the formation of α-keto acid catalyzed by $[Mo_2Fe_6S_8(SEt)_9]^{5-}$.[20] In fact, when $CH_3C(O)SPr$ was used in place of $CH_3C(O)SEt$ under the same reaction conditions, $CH_3C(O)COO^-$ was also formed with almost the same current efficiency as in the case of $CH_3C(O)SEt$.

Possible Pathway of CO_2 Fixation to RC(O)SEt. From the preceding discussion, the present CO_2 fixation is catalyzed by $[Mo_2Fe_6S_8(SEt)_9]^{5-}$. Holm et al. have revealed that terminal alkyl thiolate ligands on Fe of $[Mo_2Fe_6S_8(SR)_9]^{3-}$ can be substituted by other thiolate ligands, while thiolates bridging two molybdenums are inert to substitution reactions.[21] If the terminal EtS^- of $[Mo_2Fe_6S_8(SEt)_9]^{5-}$ is assumed to undergo such a substitution reaction by CO_2, the adduct formation may be strongly blocked by addition of an excess of free EtS^- to the solution. The CV of $(Et_4N)_3[Mo_2Fe_6S_8(SEt)_9]$ in the presence of 6 M excess of Et_4N^+ salt of EtS^- in CH_3CN, however, also showed an increase in the cathodic wave of the $[Mo_2Fe_6S_8(SEt)_9]^{4-/5-}$ redox couple at 5 mV/s under CO_2, similar to that in the absence of free EtS^- (Figure 1b). Furthermore, coordination of CO_2 to Fe of $[Mo_2Fe_6S_8(SEt)_9]^{5-}$ presumably is ruled out from a formal oxidation state of Fe(II) or Fe(III), although various η^1- and η^2-CO_2 metal complexes have been reported so far.[22,23] On the other hand, if CO_2 coordinates to $[Mo_2Fe_6S_8(SEt)_9]^{5-}$ as a Lewis acid, the electrophilic attack of CO_2 may occur at either the core, bridging, or terminal sulfur of $[Mo_2Fe_6S_8(SEt)_9]^{5-}$. It has been elucidated that not only 4Fe-ferredoxins[24] but also synthetic Fe_4S_4 clusters[25]

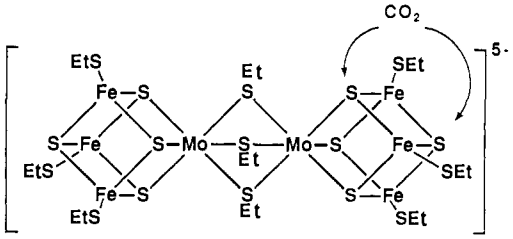

Figure 5. A possible structure of the active species.

undergo reversible protonation at core and/or terminal sulfur. For example, protonation of $[Fe_4X_4(YC_6H_4\text{-}p\text{-}t\text{-}Bu)_4]^{3-}$ (X, Y = S, Se) occurs at core sulfur and selenium with pK_a = 8.80 and 7.30 for X = S and Se, respectively, while protonation of $[Fe_4X_4(YC_6H_4\text{-}p\text{-}t\text{-}Bu)_4]^{2-}$ takes place at terminal sulfur or selenium with pK_a = 5.85 and 6.90 for Y = S and Se, respectively, in aqueous poly[2-(dimethylamino)hexanamide] solution.[26] Thus, the basicity of core sulfur of the reduced Fe_4S_4 cluster is stronger than the terminal one. Similarly, $[Mo_2Fe_6S_8X_3(SC_6H_4\text{-}p\text{-}n\text{-}C_8H_{17})_6]^{5-}$ (X = SEt and OMe) is also protonated in aqueous Triton X-100 micellar solution, and the pK_a values of those two-electron reduced MoFeS clusters are 10.8 and 10.1 for X = SEt and OMe, respectively, which are apparently larger than that of $[Fe_4S_4(SC_6H_4\text{-}p\text{-}n\text{-}C_8H_{17})_4]^{3-}$ (pK_a = 9.1).[27] The small difference in the pK_a values of SEt- and OMe-bridged $[Mo_2Fe_6S_8X_3(SC_6H_4\text{-}p\text{-}n\text{-}C_8H_{17})_6]^{5-}$ strongly suggests protonation of core sulfur rather than bridging SEt or OMe. Thus, the basicity of core sulfur of $[Mo_2Fe_6S_8(SEt)_9]^{5-}$ is considered to be stronger than that of bridging or terminal SEt. The most probable coordination site of CO_2 to $[Mo_2Fe_6S_8(SEt)_9]^{5-}$, therefore, may be one of core sulfur (Figure 5).

The above assumption reasonably explains that free EtS^- does not interfere the activation of CO_2 on $[Mo_2Fe_6S_8(SEt)_9]^{5-}$. Free EtS^-, however, strongly inhibits $RC(O)COO^-$ formation. It is worth noting that $[Mo_2Fe_6S_8(SPh)_9]^{3-}$ has essentially no ability to catalyze the reaction of CO_2 with thioesters. This may be associated with the lability of the terminal EtS^- ligand of $[Mo_2Fe_6S_8(SEt)_9]^{3-}$ compared with that of PhS^- of $[Mo_2Fe_6S_8(SPh)_9]^{3-}$, since the former is much more subject to substitution reactions than the latter. Although the CV of $[Mo_2Fe_6S_8(SEt)_9]^{3-}$ was consistent with that in the presence of $CH_3C(O)SEt$ under N_2 atmosphere (Figure 1b′), a slow substitution of EtS^- ligand on Fe by RC(O)SEt may be involved in the activated state. We, therefore, propose a possible reaction scheme for α-keto acid formation (Scheme I); CO_2 binds one of a core sulfur of $[Mo_2Fe_6S_8(SEt)_9]^{5-}$ as an electrophile, and then RC(O)SEt slowly coordinates to Fe with dissociating EtS^-, where CO_2 attached to $[Mo_2Fe_6S_8(SEt)_9]^{5-}$ may assist to weaken the Fe–SEt bond through an interaction of its oxygen with Fe. Thus, CO_2 and RC(O)SEt bounded to core sulfur and Fe of the two-electron reduced MoFeS cluster presumably combine to produce $RC(O)COO^-$ and EtS^- with generating $[Mo_2Fe_6S_8(SEt)_9]^{3-}$, which is reduced again to $[Mo_2Fe_6S_8(SEt)_9]^{5-}$ on a glassy carbon electrode. Accumulation of EtS^- in the solution apparently interferes the coordination of RC(O)SEt to Fe by blocking the dissociation of EtS^- from $[Mo_2Fe_6S_8(SEt)_9]^{5-}$. Although direct evidence for the proposed active species has not been obtained, not only the stability of $[Mo_2Fe_6S_8(SEt)_9]^{5-}$ during the electrolysis

(19) This is partly because of an irreversible reduction of $CH_3C(O)Cl$ at −1.5 V on a glassy carbon electrode in CH_3CN.

(20) $CH_3C(O)COO^-$ was not formed during the electrolysis of an CH_3CN solution containing $(Et_4N)_3[Mo_2Fe_6S_8(SEt)_9]$ and $CH_3C(O)OEt$ at −1.60 V under a CO_2 atmosphere.

(21) (a) Palermo, R. E.; Power, P. P.; Holm, R. H. *Inorg. Chem.* **1982**, *21*, 173. (b) Christou, G.; Mascharak, P. K.; Armstrong, W. H.; Papaefthymiou, G. C.; Frankel, R. B.; Holm, R. H. *J. Am. Chem. Soc.* **1982**, *104*, 2820. (c) Tanaka, K.; Nakamoto, M.; Tashiro, Y.; Tanaka, T. *Bull. Chem. Soc. Jpn.* **1985**, *58*, 316.

(22) (a) Calabress, J. C.; Herskovitz, T.; Kinney, J. B. *J. Am. Chem. Soc.* **1983**, *105*, 5914. (b) Gambarotta, S.; Arena, F.; Floriani, C.; Zanazzi, P. F. *J. Am. Chem. Soc.* **1982**, *104*, 5082.

(23) (a) Aresta, M.; Nobile, C. F.; Albano, V. G.; Forni, E.; Manessero, M. *J. Chem. Soc., Chem. Commun.* **1975**, 636. (b) Aresta, M.; Nobile, C. F. *J. Chem. Soc., Dalton Trans.* **1977**, 708. (c) Facchinetti, G.; Florani, C.; Zanazzi, P. F. *J. Am. Chem. Soc.* **1978**, *100*, 7405. (d) Alvarez, R.; Carmona, E.; Marin, J. M.; Poveda, M. L.; Gutierrez-Puebla, E.; Monge, A. *J. Am. Chem. Soc.* **1986**, *108*, 2286. (e) Bristow, G. S.; Hitchcock, P. B.; Lappert, M. F. *J. Chem. Soc., Chem. Commun.* **1981**, 1145. (f) Gambaroota, S.; Floriani, C.; Chiesi-villa, A.; Guastini, C. *J. Am. Chem. Soc.* **1985**, *107*, 2985. (g) Alt, H. G.; Schwind, K.-H.; Rausch, M. D. *J. Organomet. Chem.* **1987**, *321*, C9.

(24) (a) Skulachev, V. P. *Ann. N. Y. Acad. Sci.* **1974**, *227*, 188. (b) Prince, R. C.; Dutton, P. L. *FEBS Lett.* **1976**, *65*, 117. (c) Ingledew, W. J.; Ohnishi, T. *Biochem. J.* **1980**, *186*, 111. (d) Magliozzo, R. S.; McIntosh, B. A.; Sweeney, W. V. *J. Biol. Chem.* **1982**, *257*, 3506.

(25) (a) Bruice, T. C.; Maskiewicz, R.; Job, R. C. *Proc. Natl. Acad. Sci. U.S.A.* **1975**, *72*, 231. (b) Job, R. C.; Bruice, T. C. *Proc. Natl. Acad. Sci. U.S.A.* **1975**, *72*, 2478. (c) Tanaka, K.; Tanaka, T.; Kawafune, I. *Inorg. Chem.* **1984**, *23*, 516. (d) Tanaka, K.; Masanaga, M.; Tanaka, T. *J. Am. Chem. Soc.* **1986**, *108*, 5448.

(26) Nakamoto, M.; Tanaka, K.; Tanaka, T. *Bull. Chem. Soc. Jpn.* **1988**, *61*, 4099.

(27) Tanaka, K.; Moriya, M.; Tanaka, T. *Inorg. Chem.* **1986**, *25*, 835.

but also the inhibitory effect of free EtS^- on the formation of $RC(O)COO^-$ are well explained by Scheme I.

Registry No. CO_2, 124-38-9; AcSEt, 625-60-5; $CH_3CH_2C(O)SEt$, 2432-42-0; PhC(O)SEt, 1484-17-9; EtSH·Na, 811-51-8; $(Bu_4N)_3[Mo_2Fe_6S_8(SPh)_9]$, 68197-68-2; $(Et_4N)_3[Mo_2Fe_6S_8(SEt)_9]$, 72895-02-4; $AcCO_2^-$, 57-60-3; $CH_3CH_2C(O)CO_2^-$, 339-71-9; $PhC(O)CO_2^-$, 50572-54-8; HCO_2^-, 71-47-6; AcCl, 75-36-5; AcOAc, 108-24-7; AcSAc, 3232-39-1; AcSPr, 2307-10-0; 1-acetylimidazole, 2466-76-4; acetyl coenzyme A, 72-89-9.

Is the Vanadate Anion an Analogue of the Transition State of RNAse A?†

M. Krauss* and Harold Basch

Contribution from the Center for Advanced Research in Biotechnology, National Institute of Standards and Technology, Gaithersburg, Maryland 20899, and the Department of Chemistry, Bar-Ilan University, Ramat-Gan, Israel. *Received July 1, 1991*

Abstract: The electronic structures of models of the monoanion phosphorane transition state in ribonuclease A and its putative vanadate transition-state analogue are compared. The electrostatic potential and gross atomic populations agree well for the vanadium and phosphorus trigonal-bipyramidal transition-state structures for both equatorial and axial bonds to hydroxyl ligands but are different for the V–O and P–O bonds. The P–O bond is semiionic but V–O is a multiple bond that is much less polar. A similar difference in the polarity between P–O and V–O is found for the dianion. Ionic hydrogen bonds to the cationic residues will not be comparable between the V–O and P–O bonds. The vanadium compound is not a transition-state analogue for such H-bonds. The pattern of Lys-41 and His-12 residue bonding observed for the vanadate-inhibited RNase A should not be used to analyze the mechanism. Proton transfer between the five-coordinate transition state and the His-119 residue is a step in both the cyclization and hydrolysis phases of the mechanism. The proton transfer curve from the equatorial hydroxyl ligand to a model of His-119 is calculated to be essentially equivalent for the vanadium and phosphorus five-coordinate models of the active site. Residue binding to the vanadate monoanion would be analogous to stabilization of the transition-state intermediate. Stable vanadium dianion intermediates, which are electronic analogues of the dissociative phosphorus dianion, are calculated with both equatorial–equatorial and equatorial–axial deprotonated oxygen sites. The equatorial–axial dianion is lowest in energy and accounts for the binding of the His-119 residue in the vanadium system although the binding is weaker than for the phosphorus analogue.

1. Introduction

Ribonuclease A (RNase A) cleaves RNA by transphosphorylation and subsequent hydrolysis of the 2′,3′-cyclic phosphate intermediate. In both steps a five-coordinate phosphorane transition state is hypothesized. Vanadium can adopt a number of valence states with a variety of conformations and a uridine vanadate was proposed as a stable analogue of the transition-state complex[1] for RNase A. Subsequently, crystallographic, neutron diffraction, and NMR studies[2-4] of a complex of uridine vanadate and RNase A examined a five-coordinate vanadate at the active site and determined the protonation states of the bound residues. The Lys-41 and His-12 residues were not found in H-bonding positions expected from the presumed mechanism[1] and raised doubts on details of that mechanism. Although there is experimental evidence that the Lys-41 is flexible[3,4] in the native enzyme, another explanation for the H-bonding at the active site is possible if the vanadate(V) (designated V) does not have comparable electronic properties to the phosphorane(V) (designated P) transition state leading to different hydrogen binding behavior and orientations. The H-bonding orientation to the His-119 residue also is surprising. The His-119 residue in the uridine vanadate RNase is actually positioned closest to the equatorial oxygen. But the largest hydrogen-bonding density is reported at the axial oxygen,[2] with the distance from His-119 to the axial oxygen about 0.6 Å longer than that to the equatorial. Apparently this residue is interacting with both the axial and equatorial ligands. Analysis of the neutron scattering finds the three residues, His-12, Lys-41, and His-119, protonated in the crystal and presumably bound to the dianion, but the NMR results strongly suggest the vanadate in solution is a monoanion.[4]

Although both the P and V five-coordinate monoanions are structurally related trigonal bipyramids, the electronic differences between the valence p-oribtal in P and the d-orbital in V are substantial. Formally the two complexes can be considered to be comparable as p^0 or d^0 systems, but the calculated populations for p and d are closer to the neutral atoms. The five-coordinate vanadate is a stable molecule and an enzyme inhibitor but the analogue properties are presumed to be manifest in the position of the protons and the H-bonding to the surrounding residues.[5] This paper will examine whether the vanadium five-coordinate complex is a transition-state analogue (TSA) electronically as well as structurally by examining the comparable geometric and electronic characteristics of the five-coordinate monoanion and dianion, H_4XO_5 (X = P or V).

One test compares the electrostatic potential generated by $H_4XO_5^-$ (X = P or V) at equatorial and axial H-bonding sites that are important in binding the three cationic residues implicated in the mechanism. The similarities and differences in the electronic structure of the P and V compound are analyzed. It is well-known that the central phosphorus atom often forms bonds of an ionic or "semipolar" character.[6] The semipolar P–O bond in the phosphorane is a single ionic or dative ionic bond. This type of

†This research was supported by Grant 88-00406/1 from the United States–Israel Binational Science Foundation (BSF), Jerusalem, Israel.

(1) Lindquist, R. N.; Lynn, J. L.; Lienhard, G. E. *J. Am. Chem. Soc.* **1973**, *95*, 8762.
(2) Wlodawer, A.; Miller, M.; Sjolin, L. *Proc. Natl. Acad. Sci. U.S.A.* **1983**, *80*, 3628.
(3) Alber, T.; Gilbert, W. A.; Ponzi, D. R.; Petsko, G. A. *Ciba Found. Symp.* **1983**, *93*, 4.
(4) Borah, B.; Chen, C.; Egan, W.; Miller, M.; Wlodawer, A.; Cohen, J. S. *Biochemistry* **1985**, *24*, 2058. Brookhaven protein data bank structure 6RSA.
(5) Lolis, E.; Petsko, G. A. *Annu. Rev. Biochem.* **1990**, *59*, 597.
(6) Wallmeier, H.; Kutzelnigg, W. *J. Am. Chem. Soc.* **1979**, *101*, 2804.

0002-7863/92/1514-3630$03.00/0